

# Low-Profile and Planar Antenna Suitable for WLAN/Bluetooth and UWB Applications

Bahadır S. Yıldırım

**Abstract**—This letter presents a microstrip-fed antenna that is small, low-profile, planar, and suitable for WLAN/Bluetooth and ultrawideband (UWB) applications. The antenna occupies an area of  $16 \times 18$  (mm) on a printed circuit board (PCB) and exhibits dual-band operation at 2400–2484 MHz (Bluetooth) and 5150–5825 MHz (IEEE 802.11a and HiperLAN/2) bands with satisfactory radiation properties. The 10-dB return loss bandwidth of the antenna at high-band spans from about 4.5 GHz to about 11 GHz.

**Index Terms**—Finite-difference time-domain (FDTD), planar antennas, ultrawideband (UWB), WLAN/Bluetooth.

## I. INTRODUCTION

A LOW-PROFILE, small, planar, and dual-band microstrip-fed antenna suitable for IEEE 802.11a (5150–5350 MHz, 5725–5825 MHz), IEEE 802.11bg (2400–2484 MHz), and HiperLAN/2 (5470–5725) bands is presented in this letter. The low band of the antenna covers IEEE 802.11bg (Bluetooth) and the high band covers IEEE 802.11a and HiperLAN/2 frequencies. The microstrip-fed WLAN/Bluetooth antenna is very easy to manufacture, low-cost, and can be easily integrated within the printed circuit boards (PCBs) of notebook computers, mobile terminals, and other wireless networking equipment. Analysis of the WLAN/Bluetooth antenna is carried out using a finite-difference time-domain (FDTD) technique [1] and results are compared to that of high-frequency structure simulator (HFSS) by Ansoft for validation.

Planar inverted-F antennas (PIFA) were reported in the literature [2], [3] for WLAN/Bluetooth applications. Although PIFAs are very popular as mobile phone antennas due to their somewhat smaller dimensions and multi-band functionality, they are not suitable for wideband operations. Microstrip-fed monopole antennas were introduced for mobile handset applications [4], [5], and their proper operation requires removal of the ground metallization on the other side of the radiator. Handset PCBs are usually small, very crowded with components, and removal of large amounts of ground metallization will limit the space required for building microstrip and stripline transmission lines, and other components for the RF circuitry. However, if the radiator is very small or the PCB is very large, this may not be the issue. The miniaturized WLAN/Bluetooth antenna presented in this letter is very small and has transverse dimensions of  $16 \times 18$  (mm), excluding the region allocated for the microstrip feed

line. Since there is no ground metallization underneath the radiator, the WLAN/Bluetooth antenna can be considered as a monopole. It will be shown that UWB functionality can also be added to the miniaturized WLAN/Bluetooth antenna with a very small modification. Antennas having similar radiator patterns to the ones presented in this letter can be built on different types of microwave substrates and modified for custom applications. The ultimate performance of the antenna will be determined by its dimensions, its position on the PCB, shape of the mobile equipment and its material content, PCB dimensions, and material properties of the substrate used.

## II. MICROSTRIP-FED WLAN/BLEETOOTH ANTENNA ON FR4 SUBSTRATE

The WLAN/Bluetooth antenna shown in Figs. 1 and 2 is fed by a 2-mm-wide microstrip transmission line. The antenna provides a dual-band operation due to two different resonances generated by two different length of strips. The shorter WLAN strip is 7 mm long and is responsible for the generation of 802.11a and HiperLAN/2 (5150–5825 MHz) bands. The longer Bluetooth strip is responsible for the Bluetooth band (2400–2484 MHz) and connected to the same feed point as with the WLAN strip. The PCB is a 1.0-mm-thick FR4 substrate whose dielectric constant and loss tangent are 4.4 and 0.02, respectively with transverse dimensions of  $20 \times 40$  (mm).

A computational space of  $121 \times 161 \times 91$  cells were used for FDTD simulations, excluding the space allocated for eight-layer perfectly matched layer (PML) absorbing boundaries. Cell dimensions are selected as  $\Delta x = \Delta y = 0.5$  mm,  $\Delta z = 0.25$  mm. A time-domain Gaussian derivative pulse was used as the source of excitation. When selecting the pulse waveform in FDTD analysis, care must be given that the applied pulse has sufficient spectral energy content over the operational bandwidth of the antenna (or any other microwave device in general) in order to obtain meaningful results. The Gaussian pulse was applied at the input of the microstrip transmission line through a  $50 \Omega$  series source resistor. Energy in the computational space can be dissipated faster through the source resistor, and fewer time steps are required for the transient analysis. This is especially true in the analysis of a highly resonant structure such as a microstrip patch antenna [6]. The microstrip transmission line is driven by a source electric field  $E_z$  and the strip conductor is tapered down to the source location as shown in Fig. 3.

Time domain voltage and current at the input port are recorded during the transient simulation. Input current is calculated from the line integral of the magnetic fields around the source electric field  $E_z$ . After all transients are dissipated, time-domain voltage and current at the input port are frequency

Manuscript received May 26, 2006; revised July 27, 2006.

The author is with the Department of Electrical Engineering, Fatih University, 34500 Büyükdere, Istanbul, Turkey (e-mail: byildirim@fatih.edu.tr; bahadir.yildirim@yahoo.com).

Digital Object Identifier 10.1109/LAWP.2006.883080

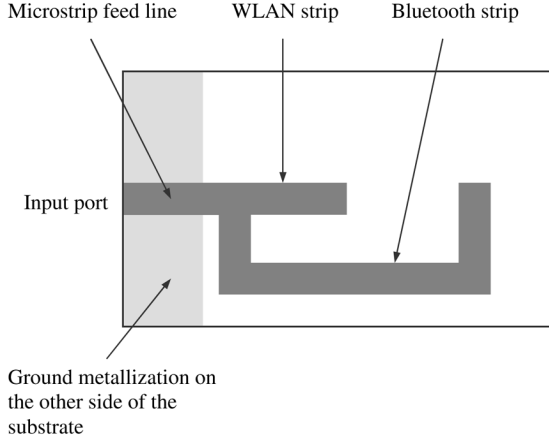


Fig. 1. Microstrip-fed WLAN/Bluetooth antenna on a  $20 \times 40$  (mm) FR4 substrate.

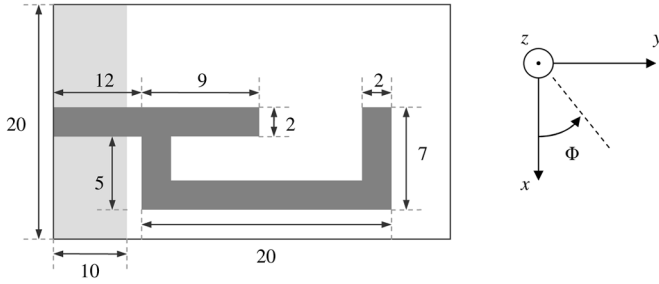


Fig. 2. All dimensions are in millimeters. The antenna is positioned in the  $x$ - $y$  plane and  $\Phi$  is the azimuth angle for gain pattern calculations.

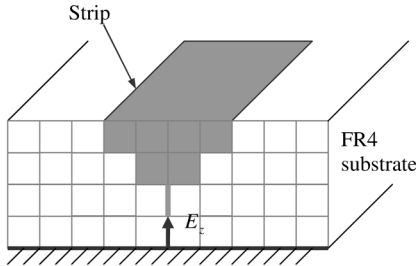


Fig. 3. Excitation of the microstrip transmission line during FDTD analysis.

transformed to obtain wide-band frequency domain response, i.e., complex input impedance and return loss. FDTD calculated return loss of the WLAN/Bluetooth antenna is shown in Fig. 4 and compared to that of HFSS for validation. The WLAN/Bluetooth antenna is well matched since the return loss is lower than  $-10$  dB at desired frequencies.

HFSS is a widely used full-wave electromagnetic solver based on a finite-element method (FEM) and solves electromagnetic fields in a computational space at each frequency point. FDTD technique solves the fields in time domain and frequency dependent antenna parameters can be calculated simply by Fourier transforming the transient data. In the analysis of ultra wide band antennas (or microwave devices), FDTD will be a better choice in terms of run time.

Both FDTD and HFSS results are in excellent agreement at low band. However, there is a very slight discrepancy between FDTD and HFSS especially as the frequency gets higher. This may be attributed to several reasons. As the operating

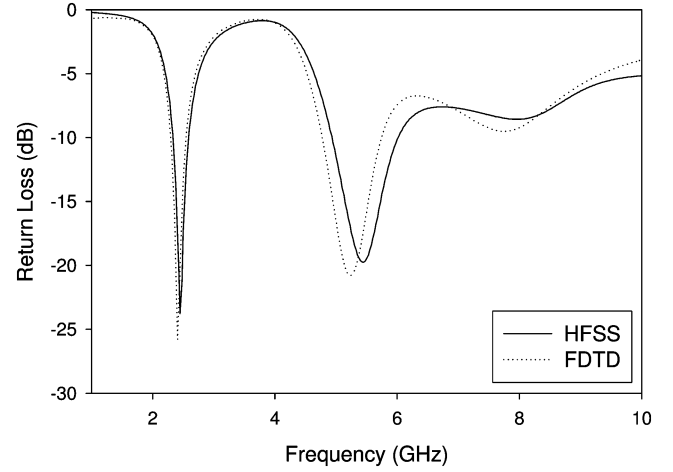


Fig. 4. Return loss of the WLAN/Bluetooth antenna on a  $20 \times 40$  (mm) FR4 substrate.

frequency increases (smaller wavelengths), resolution (cells per wavelength) of the FDTD computational space will be reduced which in turn result in numerical dispersion and reduced accuracy. Some spatial dimensions of the structure inside the FDTD computational space may be slightly smaller or larger than what they would be in reality due to the selection of cell sizes. This factor will translate to the results as shifted resonance frequency(ies).

The far-field radiation pattern is calculated when the antenna is driven by a sinusoidal source voltage. Transient input voltage and current are recorded during the simulation. When the fields achieve steady-state within the FDTD computational space, a discrete Fourier transform is performed over a virtual surface which encloses the radiating structure to calculate the far zone fields of the antenna. Once the input power and the far fields are known, efficiency and gain pattern at various planes can be computed. The WLAN/Bluetooth antenna gain pattern at 5.4 GHz is calculated using the FDTD technique at elevation plane when the azimuth angle  $\Phi$  is set to  $90^\circ$  and compared with that of HFSS as shown in Fig. 5. An excellent agreement has been achieved in the calculation of antenna gain pattern. Efficiency and the maximum gain of the antenna are calculated as 0.94 and 4.06 dBi, respectively.

### III. MINIATURIZED WLAN/BLEETOOTH ANTENNA

The antenna can be further reduced in size by folding the Bluetooth strip around the WLAN strip to shrink the overall size of the antenna, as shown in Fig. 6. New PCB dimensions are  $16 \times 28$  (mm). Substrate is still a 1.0-mm-thick FR4. The miniaturized WLAN/Bluetooth antenna is analyzed with the FDTD technique described before. A computational space of  $113 \times 137 \times 91$  cells were used in FDTD simulations, excluding the space allocated for 8-layer PML absorbing boundaries. Cell dimensions are selected as  $\Delta x = \Delta y = 0.5$  mm, and  $\Delta z = 0.25$  mm.

Return loss of the miniaturized WLAN/Bluetooth antenna is shown in Fig. 7. The antenna is well matched from 2400 MHz to 2484 MHz, and from 5150 MHz to 5825 MHz. In fact,  $-10$  dB return loss bandwidth at high band spans from about 4.5 GHz

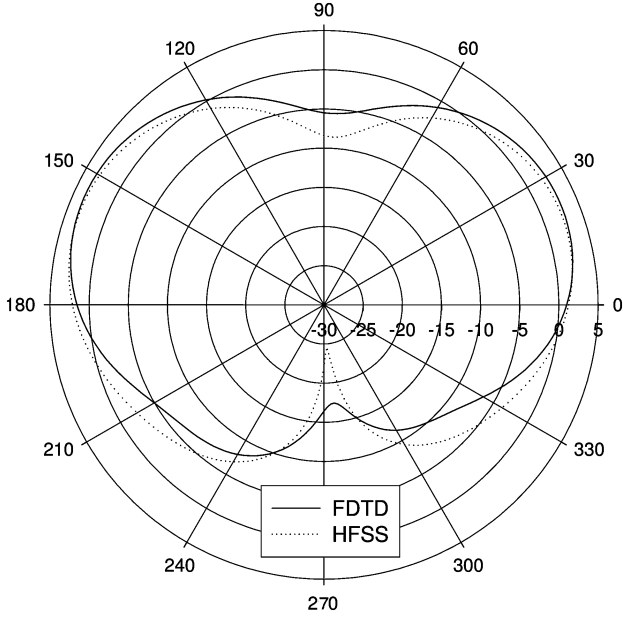


Fig. 5. Gain pattern of the WLAN/Bluetooth antenna on a  $20 \times 40$  (mm) FR4 substrate at 5400 MHz for  $\Phi = 90^\circ$ .

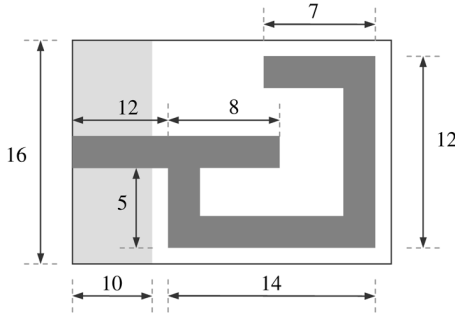


Fig. 6. Miniaturized microstrip-fed planar antenna on a  $16 \times 28$  (mm) FR4 substrate. All dimensions are in millimeters.

to all the way up to 8 GHz, which makes the upper bandwidth about 3.5 GHz. This property of the WLAN/Bluetooth antenna can be further improved to include UWB functionality as we will see Section IV.

Elevation plane gain pattern of the miniaturized WLAN/Bluetooth antenna at 5.4 GHz is calculated with the FDTD technique for  $\Phi = 90^\circ$  plane. An excellent agreement has been achieved between FDTD and HFSS as shown in Fig. 8. Efficiency and the maximum gain of the antenna are calculated as 0.95 and 2.81 dBi, respectively.

#### IV. UWB OPERATION AT HIGH BAND

In 2002, Federal Communications Commission (FCC) allocated unlicensed use of the spectrum from 3.1 to 10.6 GHz for UWB communications. Very low-Q planar and nonplanar (volumetric) UWB antennas usually have smooth structural transitions to avoid energy reflections from end-points and are discussed in [7]. Microstrip-fed small and planar UWB antennas can be easily integrated within the PCBs of various systems. An alternative technique to obtain very wide band response is to use multiple resonators having resonance frequencies somewhat close to each other. This technique will be implemented to

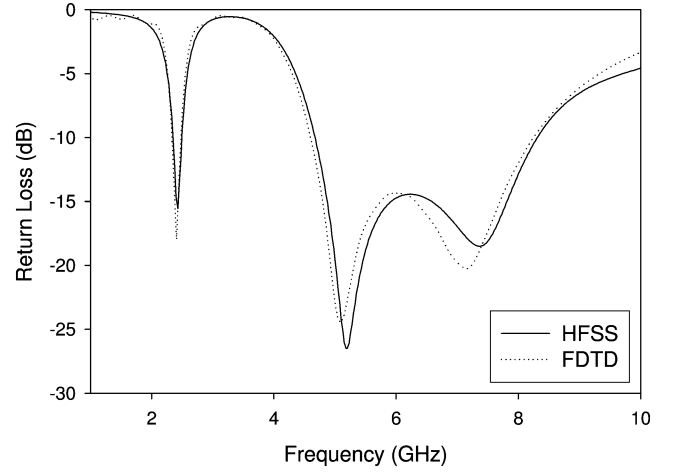


Fig. 7. Return loss for the miniaturized microstrip-fed WLAN/Bluetooth antenna on a  $16 \times 28$  (mm) FR4 substrate.

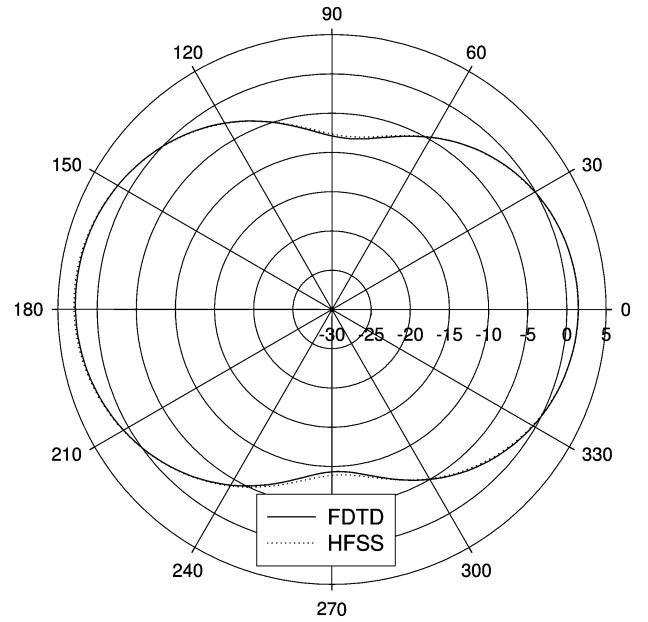


Fig. 8. Gain pattern of the WLAN/Bluetooth antenna on a  $16 \times 28$  (mm) FR4 substrate at 5400 MHz for  $\Phi = 90^\circ$  plane.

add UWB functionality for the miniaturized WLAN/Bluetooth antenna whose bandwidth at high band can be further widened by adding another radiating element as shown in Fig. 9. Let this  $3 \times 2$  (mm) element be identified as the UWB strip. When combined with the resonance of the 6 mm WLAN strip, the resonance of the UWB strip produces an effect which results in very wide high band. If the UWB strip length is too short, the two resonances would be too far from each other and the desired effect can not be observed.

Since the WLAN/Bluetooth/UWB antenna has the same physical dimensions and material parameters as with the miniaturized WLAN/Bluetooth antenna except the 3-mm-long UWB strip, FDTD analysis is carried out in a similar fashion using the same computational space and cell sizes. Calculated return loss is shown in Fig. 10. The  $-10$  dB return loss bandwidth at high band spans from about 4.5 to 11 GHz. The low end of the allocated UWB spectrum is 3.1 GHz and the miniaturized

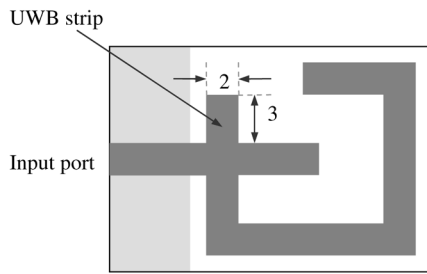


Fig. 9. A WLAN/Bluetooth/UWB antenna. The whole structure is as same as the miniaturized WLAN/Bluetooth antenna except the UWB strip. All dimensions are in millimeters.

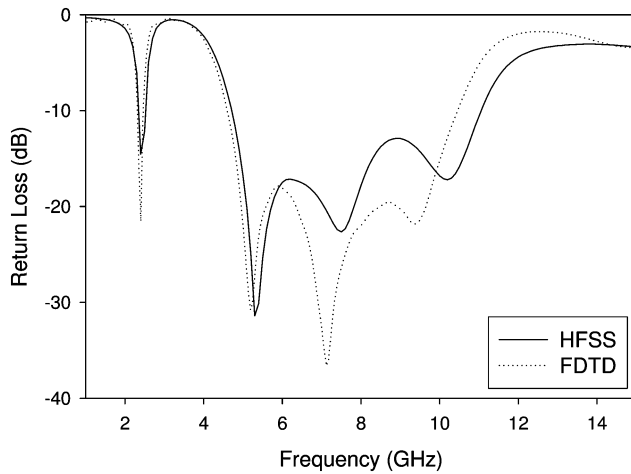


Fig. 10. Return loss for the miniaturized microstrip-fed WLAN/Bluetooth and UWB antenna.

WLAN/Bluetooth/UWB antenna can be further improved to utilize the full UWB spectrum.

## V. CONCLUSION

A small, planar, dual-band, low-cost, and easy to manufacture WLAN/Bluetooth antenna having UWB functionality is presented in this letter. The WLAN/Bluetooth antenna achieves excellent dual-band operation and can be built on other types of microwave substrates as well. It can be positioned at the edge of a PCB of a notebook computer, or any other wireless equipment. The ground metallization underneath the radiator must be cleared for proper operation. The WLAN/Bluetooth/UWB antenna return loss has to be improved so that the 3.1–10.6 GHz band allocated by FCC can be fully utilized.

## REFERENCES

- [1] K. S. Yee, "Numerical solution of initial boundary value problems involving Maxwell's equations in isotropic media," *IEEE Trans. Antennas Propagat.*, vol. 14, pp. 302–307, May 1966.
- [2] P. Nepa, G. Manara, A. A. Serra, and G. Nenna, "Multiband PIFA for WLAN mobile terminals," *IEEE Antennas Wireless Propagat. Lett.*, vol. 4, pp. 349–350, 2005.
- [3] H. Iwasaki, N. Tokairin, and K. Tamakuma, "Dual and wide band internal planar antenna for wireless LAN," in *Proc. IEEE Antennas Propagation Symp.*, vol. 4, Jun. 2004, pp. 4276–4279.
- [4] K.-L. Wong, G.-Y. Lee, and T.-W. Chiou, "A low-profile planar monopole antenna for multiband operation of mobile handsets," *IEEE Trans. Antennas Propagat.*, vol. 51, pp. 121–125, Jan. 2003.
- [5] Y.-S. Shin, S.-O. Park, and M. Lee, "A broadband interior antenna of planar monopole type in handsets," *IEEE Antennas Wireless Propagat. Lett.*, vol. 4, pp. 9–12, 2005.
- [6] R. J. Luebbers and H. S. Langdon, "A simple feed model that reduces time steps needed for FDTD antenna and microstrip calculations," *IEEE Trans. Antennas Propagat.*, vol. 44, pp. 1000–1005, Jul. 1996.
- [7] M. A. Peyrot-Solis, G. M. Galvan-Tejada, and H. Jardon-Aguilar, "State of the art in ultrawideband antennas," in *Proc. 2nd Int. Conf. Electrical and Electronics Engineering (ICEEE) and XI Conf. Electrical Engineering (CIE 2005)*, Mexico City, Mexico, Sep. 2005, pp. 101–105.